

Research Article

Identification of Prognostic Aging-Related Genes Associated with Immune Cell Infiltration in Glioblastoma

Xiaopeng Zhu,^{1,2} Xun Chen,^{2,3} Zhao Liu,⁴ Bihui Yang,⁵ Yuxiang Zhou,¹ Sian Pan,⁶ Yongkai Huang,¹ Deqing Han,¹ Yiqian Zeng ^{2,4} and Chao Liu ¹

¹Department of Neurosurgery, Zhuzhou Central Hospital, Zhuzhou, China

²Department of Trauma Center, Zhuzhou Central Hospital, Zhuzhou, China

³Department of Hepatobiliary Surgery, Zhuzhou Central Hospital, Zhuzhou 412000, Hunan Province, China

⁴Department of Critical Care Medicine, Zhuzhou Central Hospital, Zhuzhou, China

⁵Department of Hematology, Zhuzhou Central Hospital, Zhuzhou, China

⁶Department of Rehabilitation Medicine, Zhuzhou Central Hospital, Zhuzhou, China

Correspondence should be addressed to Yiqian Zeng; 124137816@qq.com and Chao Liu; 1832546464@qq.com

Received 24 September 2022; Revised 21 October 2022; Accepted 25 November 2022; Published 21 February 2023

Academic Editor: Muhammad Muddassir Ali

Copyright © 2023 Xiaopeng Zhu et al. This is an open access article distributed under the Creative Commons Attribution License, which permits unrestricted use, distribution, and reproduction in any medium, provided the original work is properly cited.

Background. Aging is recognized as a main tumor risk factor, and thus aging has become a field of interest in the tumor research field. Glioblastoma multiforme represents the most typical primary malignant intracranial tumor, particularly in the elderly. However, the association between aging-related genes (AGs) and GBM prognosis remains unknown. As a result, the primary goal of this study was to determine the association among AGs and the prognosis of GBM. **Methods.** A total of 307 human AGs were downloaded from the HAGR database, while the expression profiles of GSE4290 and GSE4412 were obtained from the GEO database. Furthermore, data on GBM expression profiles were obtained from the Chinese Glioma Genome Atlas (CGGA) database. The DEAGs that were differentially expressed among the AG and GBM gene expression profiles derived from GSE4290 were then identified, followed by functional analysis of the DEAGs. The survival-related AGs were then screened using univariate Cox regression analysis, which was used to build and validate a prognostic risk model. Furthermore, the ESTIMATE and CIBERSORT algorithms were utilized to explore the association between the survival-related AGs and the tumor immune microenvironment. **Results.** In entire, 29 DEAGs were identified in the GSE4290. This was monitored by the construction of the prognosis risk model using four DEAGs from the CGGA training set, including C1QA, CDK1, EFEMP1, and IGFBP2. Next, the risk model was confirmed in the CGGA experiment set and the GSE 4412 dataset. Results showed that C1QA, CDK1, EFEMP1, and IGFBP2 levels were remarkably higher in the high-risk score groups, and they had a good association with immune and stromal scores. **Conclusion.** A robust prognostic risk model was constructed and validated using four AGs, including C1QA, CDK1, EFEMP1, and IGFBP2, which had a close relationship with the immune microenvironment of GBM. This study offers a new reference to further explore the pathogenesis of GBM and recognize new and more effective GBM treatments.

1. Introduction

Glioblastoma multiforme (GBM) represents the most typical primary malignant intracranial tumor, particularly in the elderly [1]. The standard first-line treatment for GBM at this time involves the most extensive surgical resection along with radiotherapy and adjuvant chemotherapy [1–3]. Although considerable efforts have been made in the dealing of GBM in current years, the prognosis is still poor [4]. A

previous study reported that the median survival time is only about one year, and about 5% of people survive for five years overall [5]. The patients' age has been measured as a major prognostic factor for clinical outcomes [6]. Recent statistics indicate that the percentage of elderly patients with GBM is up to 25%, which can be attributed to the gradual expansion of the digits in advanced aging patients [6]. However, the exact molecular pathogenesis of GBM in elderly patients has not yet been fully elucidated. As a result, more research on

this disease is needed to predict therapeutic efficacy and guide clinical treatment decisions.

Notably, ageing is recognized as a major tumor risk factor, and thus ageing has become a focus in tumor research [7]. Many studies indicate that aging and aging-related diseases are mainly regulated by AGs which can suppress tumors through modulation of tumor cell senescence but may also enhance tumor enlargement, invasion, and metastasis [7]. However, the association between AGs and GBM prognosis has received little attention. Furthermore, there is no clear relationship between inflammation and tumor immunity in GBM. To address the essential issue of genomic erosion, a sophisticated network of DNA damage response (DDR) systems has been developed.

Cell-cycle checkpoint pathways, damage tolerance mechanisms, and DNA repair mechanisms are a few of them [8].

The HAGR is an important database for human aging-related gene expression studies. The value of AGs as prognostic factors for GBM patients was assessed in this research. The aging-related gene expression profiles were obtained from HAGR, while the GBM expression profiles were derived from the CGGA database. The main aim of this study was to elucidate the association between AGs and the prognosis of GBM by constructing a prognostic risk model. Meanwhile, the study also investigated the effects of AGs on GBM-related inflammation and immunity.

2. Methods

2.1. Acquisition of Data. All gene expression profiles were obtained from three public databases: the HAGR (HAGR, <https://genomics.senescence.info/genes/>), the GEO S (GEO, <https://www.ncbi.nlm.nih.gov/gds>), and the (CGGA) database (CGGA, <https://www.cgga.org.cn/>). A total of 307 human AGs was downloaded from the HAGR, and the GEOquery package was used to access the expression profiles of GSE4290 and GSE4412 from the GEO database. The GSE4290 dataset contained 81 GBM samples, while the GSE4412 dataset contained 85 GBM samples and was used as an independent verification group. Moreover, the GBM appearance profile statistics were downloaded from the CGGA database. An entire set of 406 GBM samples with continuation information were acquired from the CGGA database and randomly allocated into two groups using a 7 : 3 ratio: the GBM training set ($n = 284$) and the GBM test set ($n = 122$). R software (version 3.6.3, <https://www.r-project.org/>) was utilized to analyze the data.

2.2. Analysis of Differentially Expressed AGs (DEAGs). The R package limma was used to identify the DEAGs between the AGs and the GBM gene expression profiles derived from GSE4290. $|\text{LogFC}| > 1.5$ and false finding rate (FDR < 0.05) were set as the cut-off value. Finally, the DEAGs were visualized by a volcano plot using the ggpolt2 R package.

2.3. GO and KEGG Pathway Analyses. Pathway enrichment analyses using the gene ontology (GO) and KEGG databases

were conducted using the cluster Profiler R package with a cut-off criterion of p value and FDR value < 0.05 to investigate the gene function of the DEAGs. Biological processes (BP), cellular components (CC), and molecular functions make up the three categories that make up GO (MF).

2.4. Construction of a Prognostic Gene Signature. To further screen DEAGs related to survival, univariate cox regression evaluation was used. Notably, the candidate prognostic genes were chosen using the 0.05 p value threshold. Next, in the CGGA training set, LASSO regression analysis was used. The risk score was designed using the regression coefficient of each gene according to the following formula:

$$\text{Risk score} = \sum_{k=1}^n \text{coefficient}(\text{gene}_k) * \text{Exp}_k. \quad (1)$$

In the above formula, “ n ” indicates the number of the selected prognostic genes, “ gene_k ” is the k th selected genes, “coefficient” represents the estimated regression coefficient of genes from the multivariate Cox regression analysis, and “ Exp_k ” indicates the expression value of the k th selected genes. The GBM training set retrieved from the CGGA database was then dichotomized into a high-risk and low-risk groups according to the median risk score. A heatmap was used to show the relationship between candidate genes and risk scores, and Kaplan–Meier (KM) survival analysis and receiver operating characteristic (ROC) curve analysis were used to evaluate the risk score model’s predictive power.

2.5. Gene Set Variation Analysis. The nonparametric, unsupervised technique for enriching gene sets is called gene set variation analysis (GSVA). The CGGA dataset was subjected to GSVA using the GSVA R package to score the high-risk and low-risk groups in order to compare the signaling pathway activity between the two groups. In addition, gene-set enrichment analysis was used to pinpoint changes in gene expression at the pathway level in order to evaluate the biological utility of the risk model. The Molecular Signatures Database v7.0 was used for running GSVA within the hallmark gene sets.

2.6. Evaluation of Immune Scores and Immune Cell Infiltration. The ESTIMATE algorithm and the estimate R package were used to determine the immune and stromal scores for GBM samples. In addition, we imputed the composition of immune cell infiltration in GBM through the CIBERSORT algorithm. It is worth noting that CIBERSORT provides a tool that is able to quantify the abundance of cell types in complex tissues using gene expression data [9].

2.7. Statistical Analysis. R version 3.6.3 was utilized to conduct the statistical investigation. While survival statistics were conducted using the Kaplan–Meier curve and log-rank test, differences in the distribution of the Chi-square test or

Fisher's exact tests were used to compare categorical data. The association between prognostic AGs and survival in GBM patients was also examined using univariate and multivariate Cox regression analysis. ROC curves were applied to validate the diagnostic value of the risk model, and the correlation between variables was determined using Spearman's rank correlation test. $p < 0.05$ was recognized to be statistically significant.

3. Results

3.1. Analysis of DEAGs in GBM Samples. In entire, 307 human AGs were downloaded from the HAGR, and the AGs were recognized using the gene expression profile of GSE4290. The GSE4290 contained 29 DEAGs, of which 22 were upregulated and 7 were downregulated, according to the results. In order to see the DEAGs, a volcano plot was used (Figure 1(a)).

3.2. Functional Analysis of DEAGs. The biological functions and association of DEAGs in GSE4290 were explored using GO and KEGG pathway analysis. Figure 2(b) shows the top

30 KEGG enrichment terms. Functional analysis indicated that the DEAGs were enriched in cellular senescence, microRNAs in cancer, cell cycle, and other diverse tumor-associated pathways. Figure 2(a) shows the top 10 improved GO terms, including BP, CC, and MF. Notably, aging and cell aging were significantly developed in the GO BP terms. These results suggest that the DEAGs are intimately related with aging and tumor.

3.3. Identification of a Prognostic Risk Model in the CGGA Training Set. The univariate Cox regression analysis method was used to analyze the expression of the 29 DEAGs identified from the CGGA training set to assess the prognostic value of DEAGs in GBM (Figures 1(c) and 1(d)). Results represented in the forest plot showed that four DEAGs were significantly associated with the survival time, including C1QA, CDK1, EFEMP1, and IGFBP2 (Figure 1(b)). Regarding that, LASSO regression was utilized to develop a prognostic risk technique for the four survival-associated DEAGs. The resulting formula was used to analyze the prognostic risk score:

$$\text{Risk score} = 0.143 * \text{C1QA} + 0.223 * \text{CDK1} + 0.118 * \text{EFEMP1} + 0.152 * \text{IGFBP2}. \quad (2)$$

Based on their median risk scores, the patients in the CGGA training set were then categorised as high-risk or low-risk. Patients in the low-risk group had better overall survival (OS) than those in the high-risk group, according to the results of the survival analysis ($p < 0.001$, Figure 3(a)). The AUC (area under the ROC curve) of the prognostic model was 0.747, 0.843, and 0.837 for the 1-, 3-, and 5-year OS, respectively, indicating a robust performance for survival prediction (Figure 3(b)). Figure 4(a) shows the risk plot for both high- and low-risk score groups, patient survival data, and gene expression information for the risk genes.

3.4. Verification of the Prognostic Risk Model in the Validation Datasets. The prognostic risk method was tested using CGGA test data to further validate its stability and reliability. Similarly, the GBM test set of the CGGA database was specified into either high-risk ($n = 61$) or low-risk ($n = 61$) groups. The K-M survival curve suggested that the overall survival (OS) of patients in the low-risk set was superior compared to those in the high-risk group ($p < 0.001$, Figure 3(c)). The AUC for the GBM test set was 0.681, 0.785, and 0.738 for the 1-, 3-, and 5-year OS, respectively, indicating great performance for survival prediction (Figure 3(d)). Figure 4(b) shows the risk distribution, patient survival status, and gene expression data of the risk genes in the CGGA test. Furthermore, the stability and reliability of the prognostic risk model were validated using an independent dataset, the GSE4412 dataset retrieved from the GEO database. The same risk model was applied, and the GBM test set obtained from the GEO was split into two

groups: high-risk ($n = 43$) and low-risk ($n = 42$). Results showed significant differences in the overall survival (OS) of patients between the low-risk group and the high-risk group ($p < 0.001$, Figure 3(e)). Moreover, the AUC was 0.725, 0.808, and 0.793 for the 1-, 3-, and 5-year OS, respectively (Figure 3(f)). The corresponding risk distribution, patient survival status, and gene expression data of the risk genes in the GSE4412 test set are displayed in Figure 4(c).

3.5. GSVA of Risk Score-Related Signaling Pathways. GSVA was conducted to assess potential functional enrichment in the high-risk and low-risk groups in the CGGA dataset. Figure 5 shows the top 10 signaling pathways developed in the high-risk group, including angiogenesis, coagulation, epithelial-mesenchymal transition, hypoxia, IL-6/JAK/STAT3 signaling, provocative response, interferon-gamma response, and beta signaling. Most of them are common signaling pathways in the tumor immune microenvironment, metabolism, and progression.

3.6. Association between the Risk Score and Tumor Immunity. The immune and stromal scores in the CGGA and GSE4412 datasets, respectively, were computed using the ESTIMATE algorithm to clarify the association between the risk score and the immune/stromal score. The low-risk group had better immune scores than the high-risk group, according to the findings (Figures 6(a) and 7(a)). Moreover, Spearman's rank test results showed significant positive correlations among the risk score and immune score in CGGA and GSE4412 samples (Figures 6(b) and 7(b)). Meanwhile, the

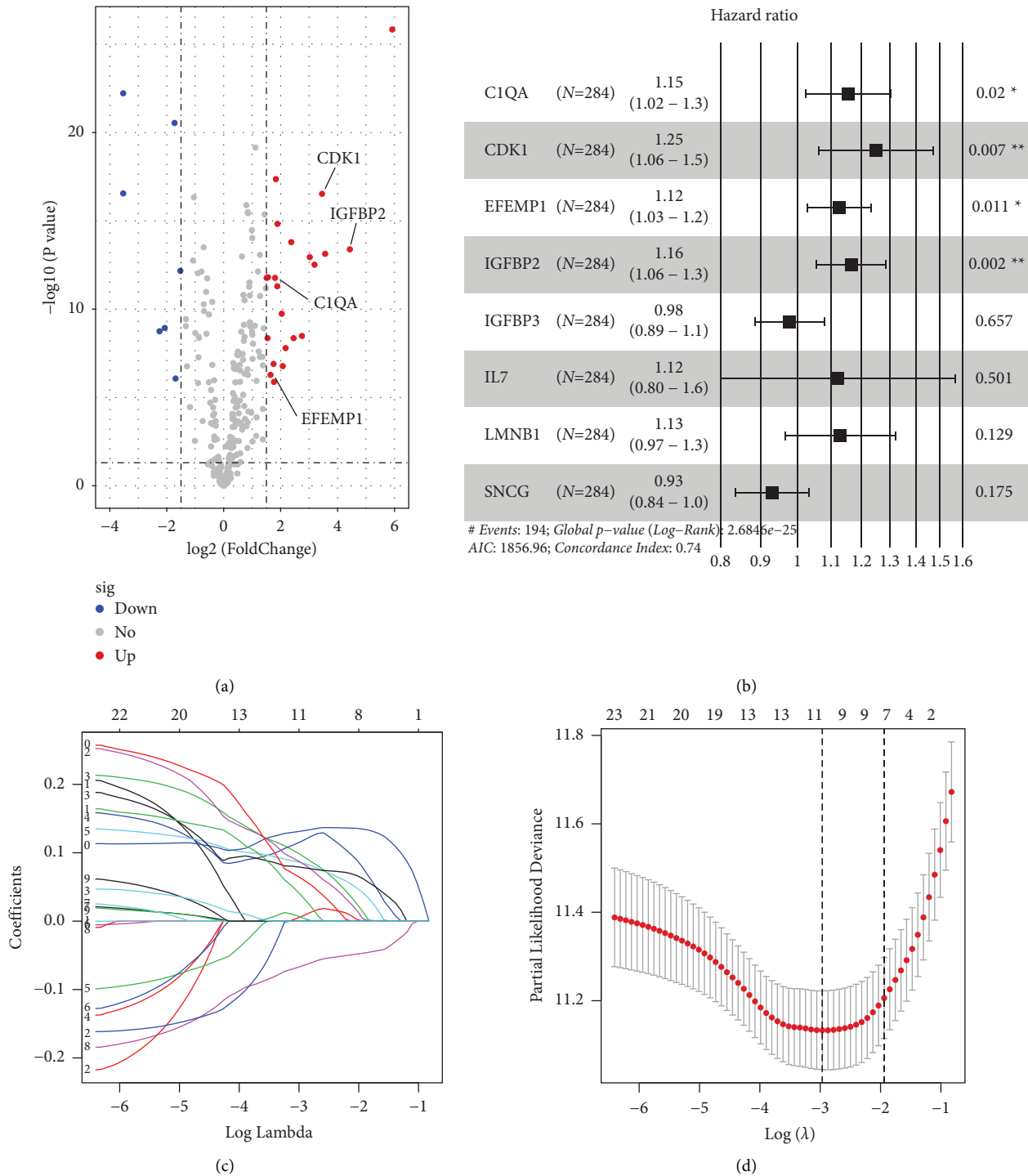


FIGURE 1: Identification of DEAGs related to GBM and 4 AGs of prognostic risk models in GBM patients. (a) 22 upregulated and 7 downregulated DEAGs in volcano plot (FDR < 0.05 and |logFC| > 1). (b) Forest plot for the characteristics of 4 risk DEAGs in the prognostic risk models. (c) LASSO coefficient profiles of candidate prognostic-related AGs. The coefficient profile plot was generated versus the log (λ). (d) Partial likelihood deviance map for the LASSO coefficient profiles.

risk score also had a significantly positive association with the stromal score and ESTIMATE score in CGGA and GSE4412 samples (Figures 6(c), 6(d), 7(c), and 7(d)). Considering that immune cells include many different subtypes, CIBERSORT was used to deconvolute the

composition fraction of immune cells in the CGGA dataset. In order to evaluate the relevance, the proportions of immune cells in the low-risk and high-risk groups were compared. According to the findings, the low-risk group had a higher percentage of naive CD4⁺ T cells, regulatory T cells

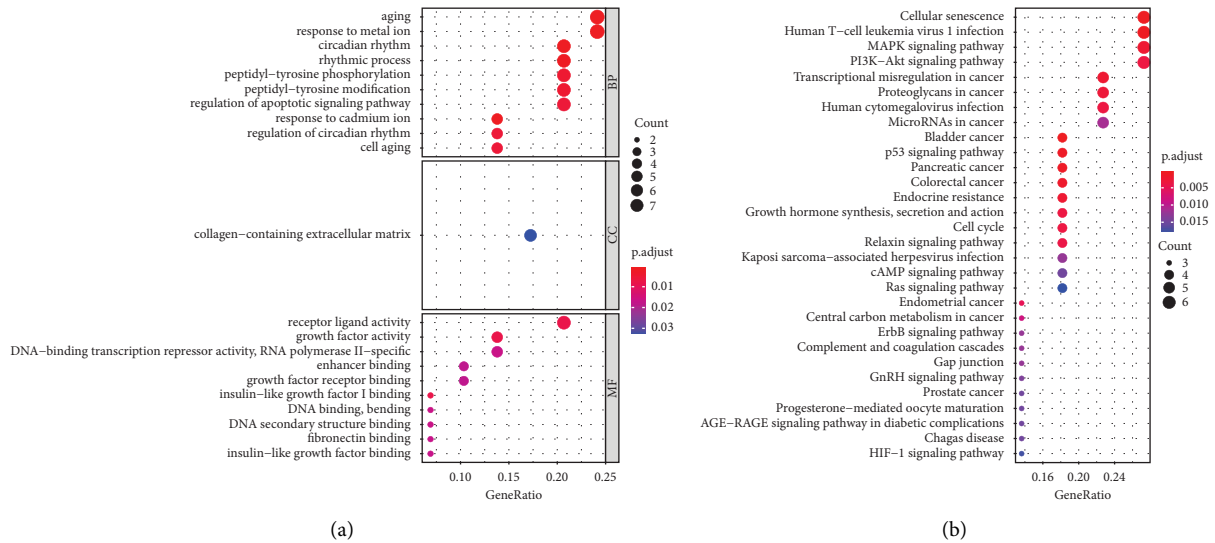


FIGURE 2: Functional enrichment analysis of DEAGs of the GSE4290 dataset. (a) The top 10 enrichment GO terms of BP, CC, and MF for DEAGs. (b) The top 30 enrichment pathways from KEGG pathway analysis for DEAGs.

(Tregs), gamma delta T cell monocytes, and activated mast cells than the high-risk group did (Figure 7(e)). Instead, fewer neutrophils, follicular helper T cells, M0 and M1 macrophages, and stimulated NK cells were present in the low-risk group compared to the high-risk group.

4. Discussion

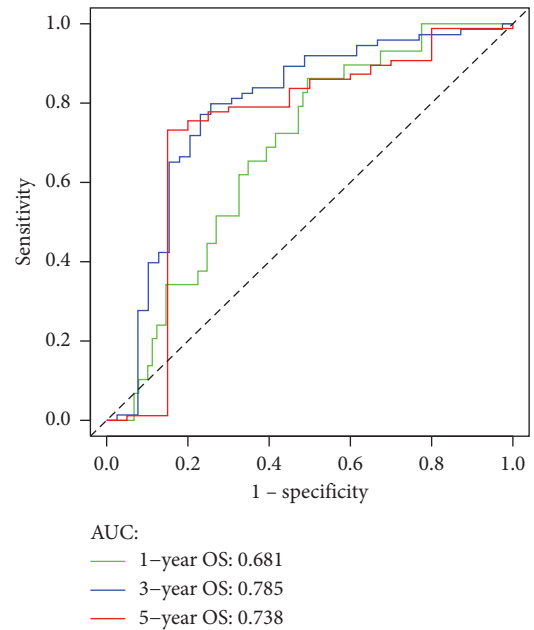
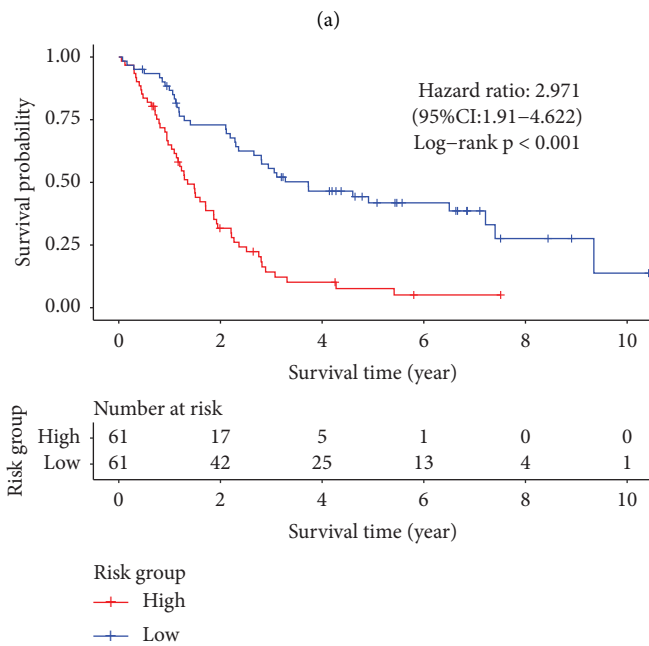
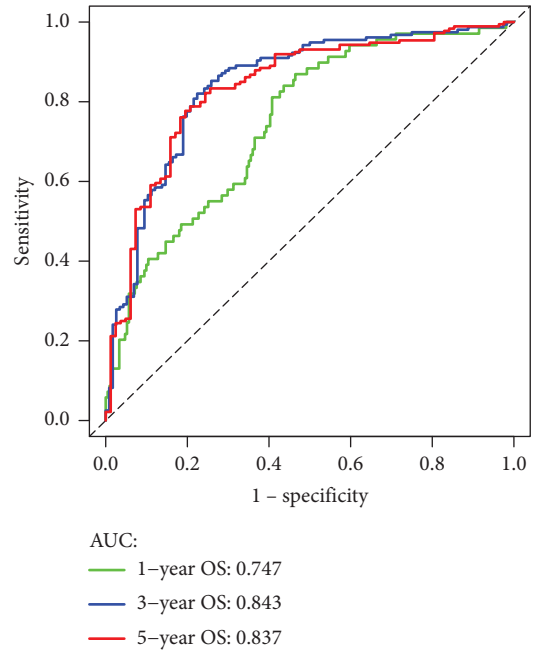
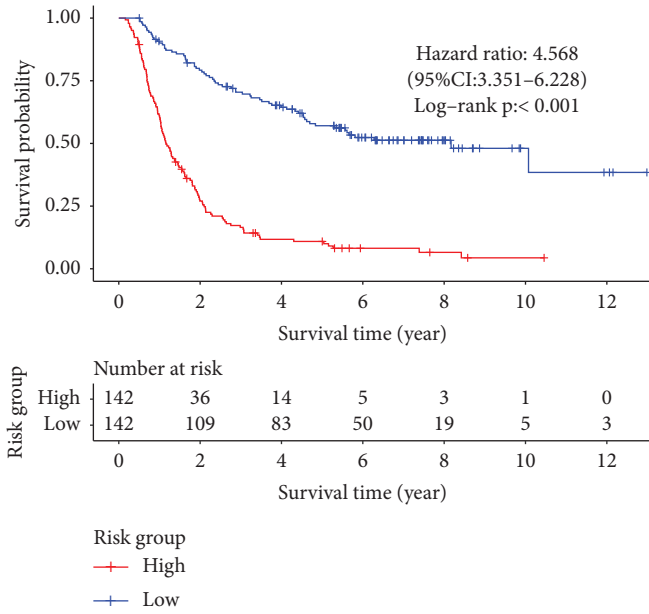
Aging is a complex natural procedure, which involves aging-related immune remodeling and dysfunction [10]. It is worth noting that the incidence of tumors increases significantly with age, which can be attributed to a decline in immune function [11]. To date, the technique of aging in GBM has not yet been fully illuminated, and there are no corresponding studies in such patients [7]. Therefore, studies should be conducted to determine the role of AGs in GBM and explore the association of AGs with the prognosis of GBM.

This study identified the relationship between 29 DEAGs (Figures 1(a) and 1(b)) and GBM prognosis, and assembled a risk model with four DEAGs, including C1QA, CDK1, EFEMP1, and IGFBP2 to predict GBM prognosis. Following that, the model's prognostic value was determined using training and independent validation cohorts, with the results demonstrating a valid and robust performance for survival prediction. C1QA, CDK1, EFEMP1, and IGFBP2 were all significantly upregulated in high-risk score groups, which means that these patients have a worse prognosis.

The C1QA gene, which encodes the C1q protein in macrophages, dendritic cells, and THP1 cells, has been implicated in the aging response and is involved in some neurodegenerative diseases [12]. Interestingly, increased gene expression of C1QA has been proven to cause a high inflammatory state in the brain of people with psychosis [13]. In addition, a previous study concluded that increased C1QA expression may facilitate tumor progression and contribute towards an adverse outcome [8]. CDK1

participates in the regulation of the G2/M phase of the cell cycle [14]. Furthermore, CDK1 is frequently overexpressed in many human malignant tumor tissues, and it has been investigated as a PB for a variety of tumors. Over-expression of CDK1 in glioma and GBM cells contributes to glioma cell senescence escape and growth [15]. As a result, CDK1 has been proposed as a promising therapeutic target. Previous research has found that EFEMP1, also known as fibulin-3, is involved in ageing, age-related diseases, and tumor formation [16, 17]. EFEMP1 knockout mice aged faster and lived shorter lives. However, previous research on the role of EFEMP1 in GBM has been inconsistent. On the one hand, some studies have shown that it has an antitumor effect by inhibiting glioma growth [18]. On the other hand, some studies found that over-expression of EFEMP1 may enhance glioma growth and contribute to resistance through the influence of multiple oncogenic waving pathways, such as Notch, AKT, and EGFR waving pathways [19, 20]. Results obtained in this study are consistent with the latter conclusion. However, this shows that more studies are essential to clarify the function of EFEMP1 in the pathogenesis of GBM. It has been informed that IGFBP-2 appearance is expressively increased after 50 years of age [21]. Moreover, several studies have indicated that there is an expressively positive correlation between IGFBP-2 concentrations and mortality in healthy elderly populations [22, 23]. Over-expression of IGFBP-2 has also been found in GBM and many other types of human tumors [24–26]. Unfortunately, the high expression of IGFBP-2 was strongly associated with a significant shortening of survival, which is consistent with the results of this study [27, 28]. Therefore, most of the existing studies propose using IGFBP-2 as a biomarker or potential novel target for GBM treatment [29, 30].

For the first time, a GBM prognostic risk model based on four AGs was developed in this study. Subsequent GSEA analysis disclosed that the risk genes' signaling pathways are elaborated in immunomodulatory and inflammatory



(a)

(b)

(c)

(d)

FIGURE 3: Continued.

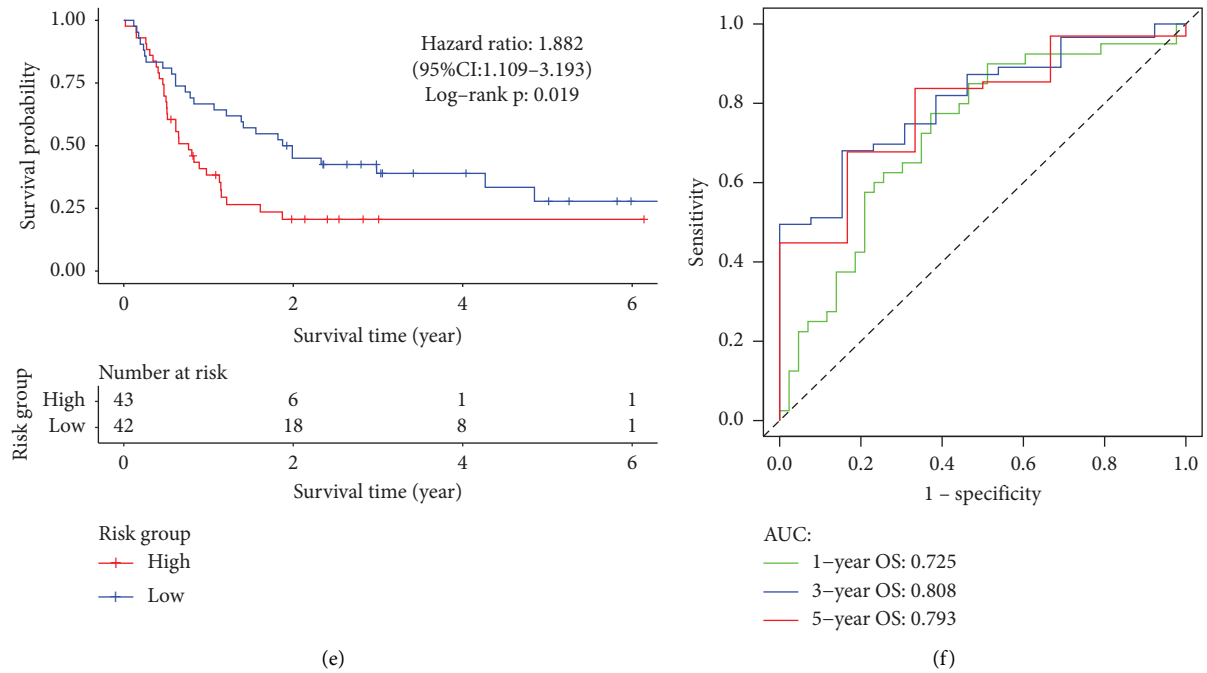


FIGURE 3: Identification and verification of the prognostic risk model in GBM. (a) Kaplan–Meier survival analysis of high-risk and low-risk groups in the CGGA training set. (b) Time-dependent ROC curves for 1-, 3-, and 5-y OS in the CGGA training set. (c, e) Kaplan–Meier survival analysis of high-risk and low-risk groups in the CGGA test set and GEO test set, respectively. (d, f) Time-dependent ROC curves for 1-, 3-, and 5-y OS in the CGGA test set and GEO test set, respectively.

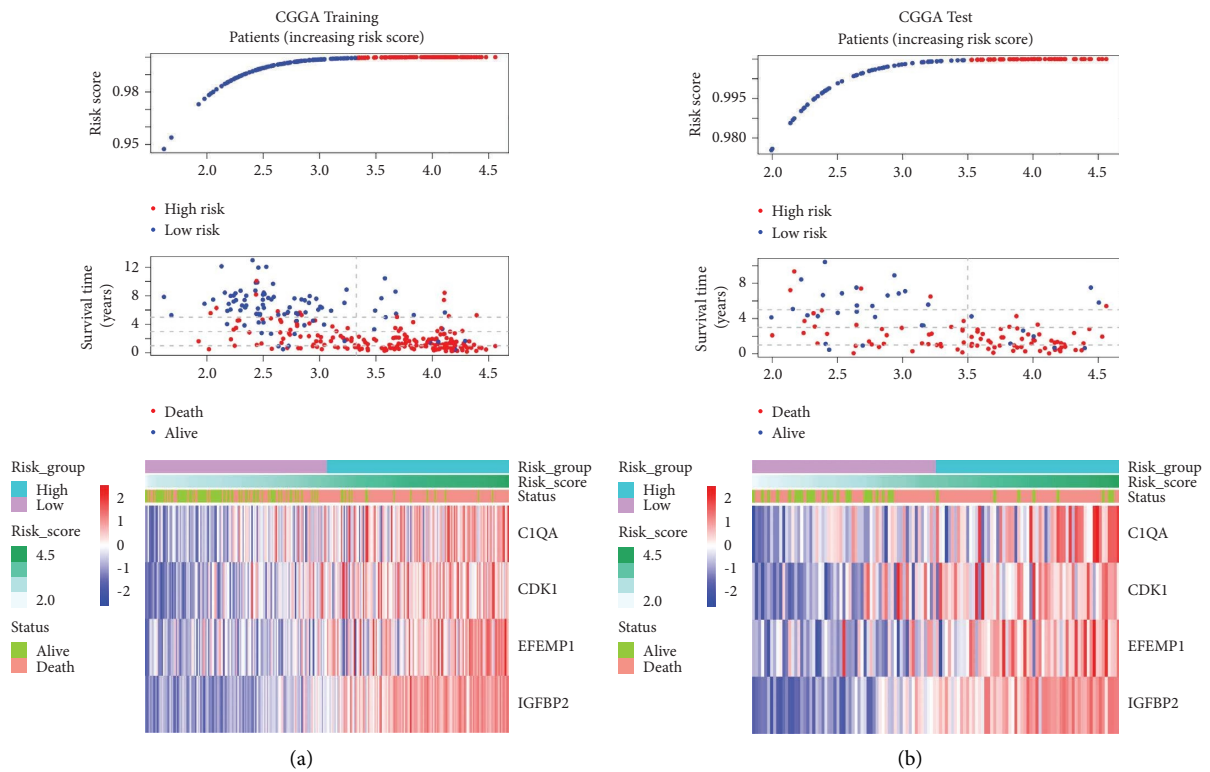


FIGURE 4: Continued.

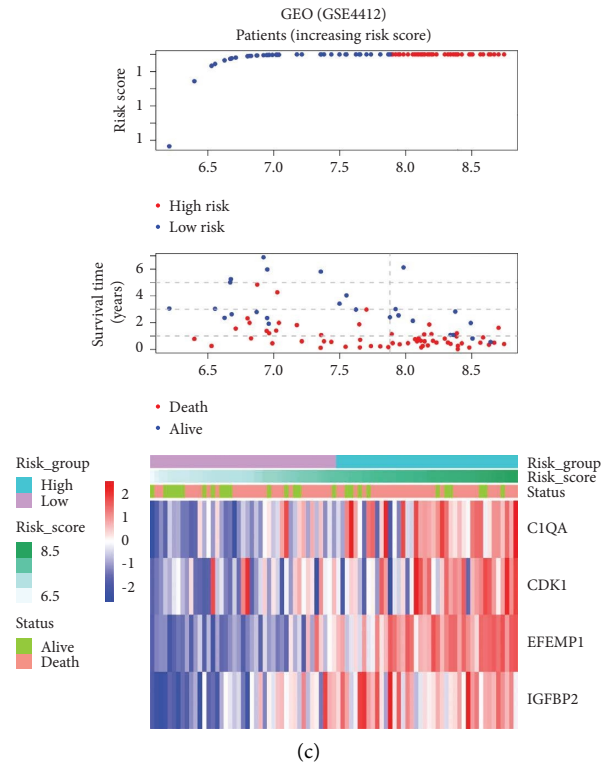


FIGURE 4: Prognosis and expression of risk genes of the high-risk and low-risk GBM patients. (a) Risk plot distribution, survival status, and risk gene expression in the CGGA training set. (b) Risk plot distribution, survival status, and expression of the risk genes in the CGGA test set. (c) Risk plot distribution, survival status, and expression of the risk genes in the GEO test set.

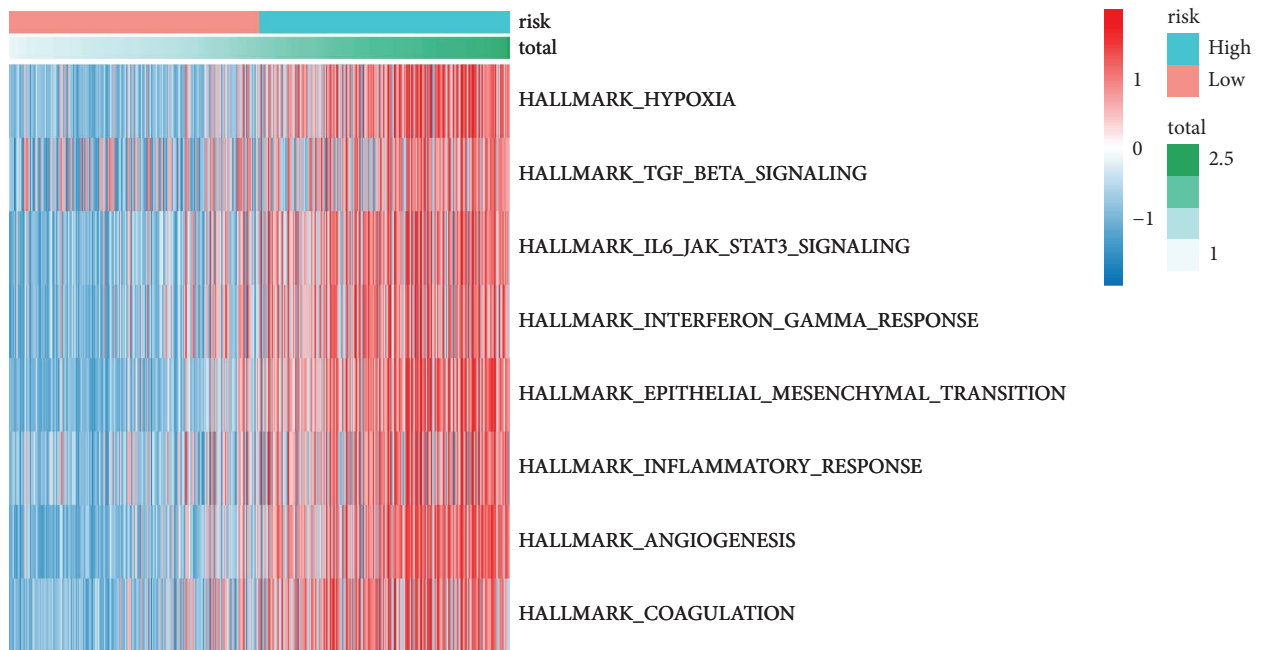


FIGURE 5: The top 10 enriched pathways of the risk gene in high-risk and low-risk groups through GSVA.

responses. The results strongly suggested a relationship between the risk genes and the GBM immune microenvironment. Based on the above findings, we further explored

the relationship among the risk score and immune score and deconvoluted the conformation fraction of immune cells in the CGGA data set and GSE4412 data set. The immune and

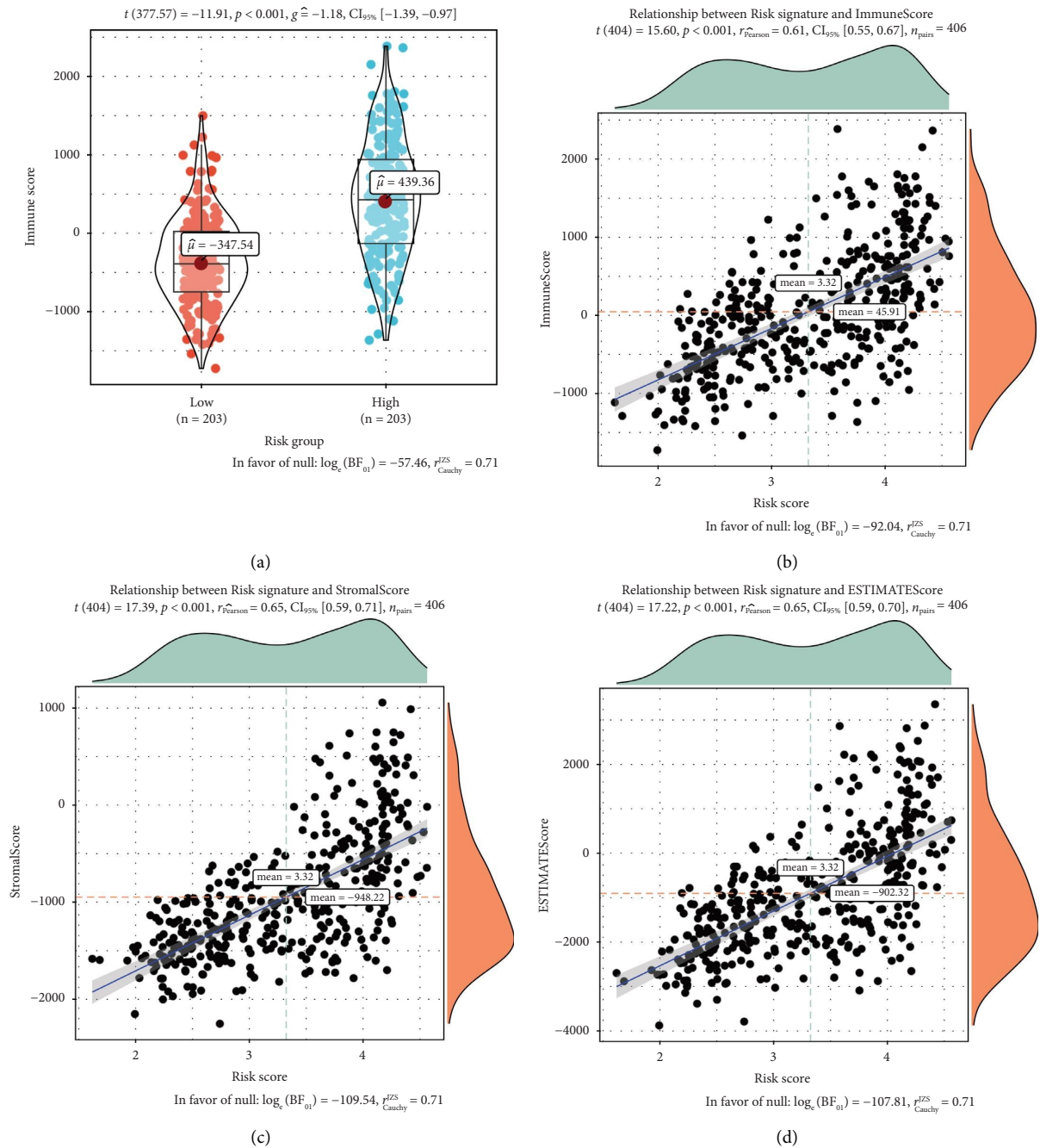
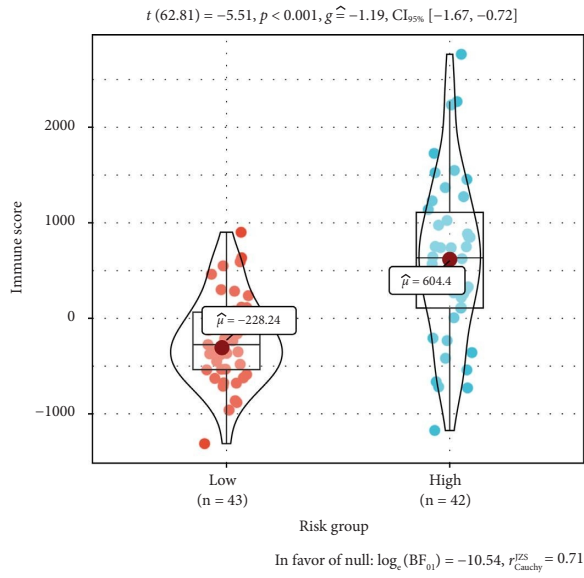


FIGURE 6: Correlation between the risk score and tumor immunity in the CGGA data set. (a) Comparisons of the immune scores in high-risk and low-risk GBM patients. (b) Association among the risk score and the immune score in GBM samples. (c) Association among the risk score and the stromal score in GBM samples. (d) Association among the risk score and the ESTIMATE score in GBM samples.

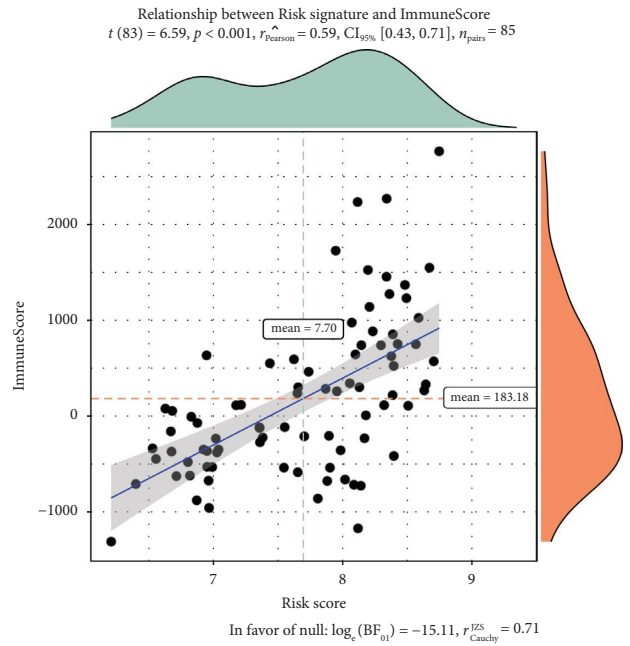
stromal scores were found to be positively associated with the risk score. This implies that the higher the immune and stromal scores, the greater the immune cell infiltration and the worse the prognosis. Recent studies have proposed that the immune score serves as an important prognostic factor of GBM. Furthermore, this study analyzed the GBM data using the CIBERSORT algorithm in order to investigate the compositional differences of 22 immune cell types based on the risk model. The findings showed that the high-risk group's NK cells, M0 macrophages, M1 macrophages, and

neutrophils were activated by the infiltration of follicular helper T cells and suggested a poor prognosis. On the other hand, the infiltration of naive CD4⁺ T cells, regulatory T cells (Tregs), gamma-delta T cells, monocytes, and activated mast cells in the low-risk group suggested a relatively good prognosis in GBM patients.

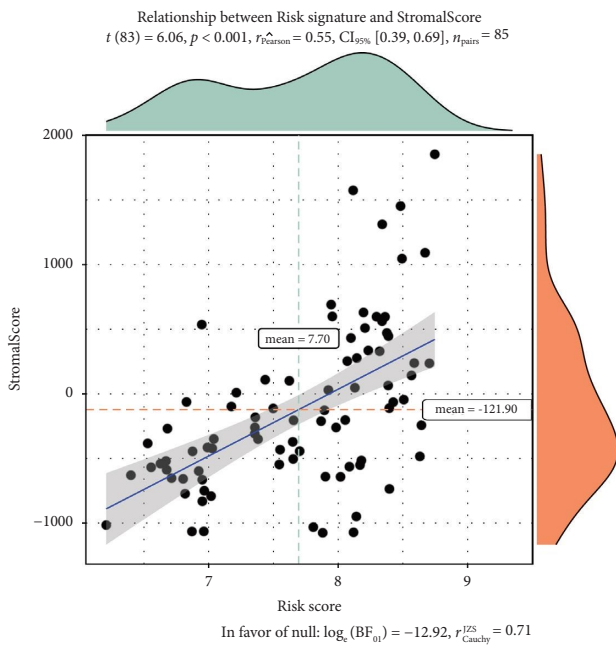
Notably, macrophages are the most abundant tumor immune infiltration cell types in human GBM. Macrophages have two main phenotypes, M1 and M2, which are differentiated from untreated macrophages (M0). Several



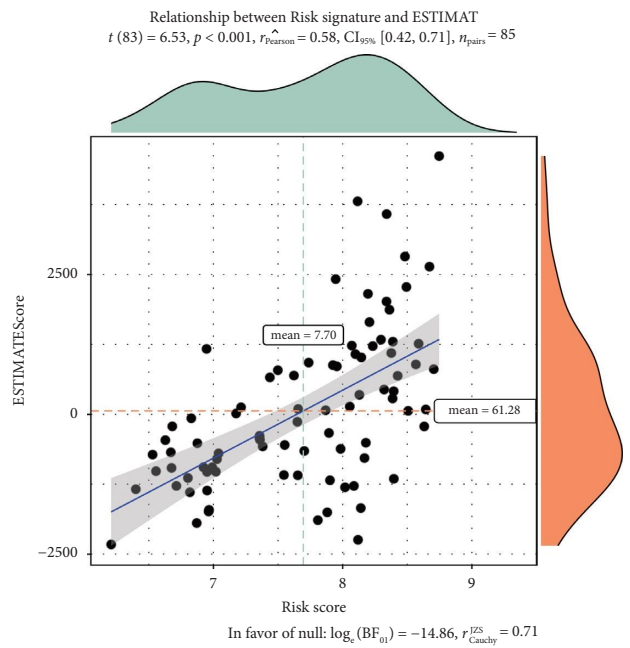
(a)



(b)

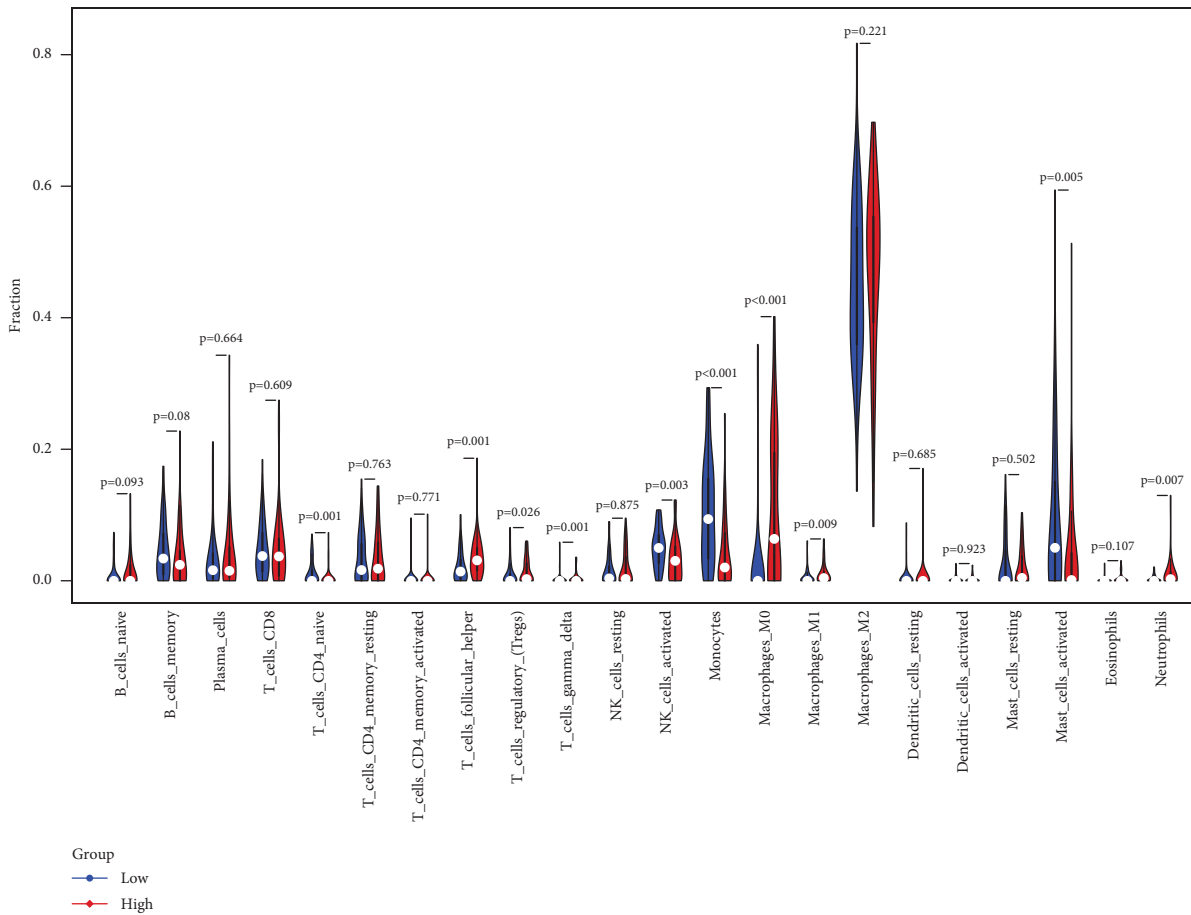


(c)



(d)

FIGURE 7: Continued.



(e)

FIGURE 7: Correlation between the risk score and tumor immunity in the GSE4412 data set. (a) Comparisons of the immune scores in high-risk and low-risk GBM patients. (b) Association among the risk score and the immune score in GBM samples. (c) In GBM samples, there is an association between the risk score and the stromal score. (d) Association among the risk score and the ESTIMATE score in GBM samples. (e) Comparisons of the fractions of 22 types of immune cells among the high-risk and low-risk groups in the CGGA data set.

previous studies indicate that M1 macrophages can perform antitumorigenic functions, whereas M0 and M2 macrophages can perform protumorigenic functions [12, 31, 32]. Despite the fact that M1 macrophages have proinflammatory and antitumor effects, a previous study found that they were inversely related to survival in GBM patients [33]. This study has shown that the proportion of M0 and M1 macrophages was significantly higher in the high-risk group than in the low-risk group. Therefore, more comprehensive and in-depth studies should be conducted to elucidate the mechanism of action of macrophages in GBM.

The role of monocytes and mast cells in tumor development and progression has previously been established. Nonetheless, the interactions of monocytes and mast cells in the tumor microenvironment are complex and contradictory [34, 35]. This study has shown that monocytes and activated mast cells were significantly lower in the high-risk group. NK cells are capable of directly killing tumor cells [36]. Although it has great cytotoxicity, the proportion of NK cells was low in the GBM immune microenvironment [37]. Interestingly, a previous study found that NK cell

deficiency in GBM improves prognosis, which is in line with our results [38]. With regard to T cells, CD4⁺ T cells seem to play a dual role in tumor immunity, while follicular helper T cells and gamma-delta T cells are relatively good prognostic signatures. The results obtained in this study are in accordance with the above-mentioned conclusions, with the exception of follicular helper T cells [39–42]. Accumulating evidence suggests that regulatory T cells are involved in immunosuppression and are associated with tumor escape and tumor progression, which is unfavorable for the outcome [43, 44]. Therefore, this discrepancy with our results should be explored more intensively. Overall, the occurrence and development of GBM involve a complex immune microenvironment [45], and thus more research is needed to explore the complex tumor immune relationships.

This study had some limitations as well. Although there was a correlation among the four AGs and the tumor immune microenvironment, further experimental verification is needed to assess the robustness of the prognostic risk model. Future studies should investigate how the four genes are elaborated in the regulation of tumor immunity.

In conclusion, a robust prognostic risk model was constructed and validated using four AGs, including C1QA, CDK1, EFEMP1, and IGFBP2, which had a close relationship with the immune microenvironment of GBM. This study offers a new reference to further explore the pathogenesis and identify new and more effective GBM treatments.

Data Availability

The data used to support the findings of this study are available from the corresponding author upon reasonable request.

Additional Points

Reporting Checklist. The authors have completed the TRIPOD reporting checklist.

Ethical Approval

The authors are accountable for all aspects of the work in ensuring that questions related to the accuracy or integrity of any part of the work are appropriately investigated and resolved.

Conflicts of Interest

All authors have completed the ICMJE uniform disclosure form. The authors declare that they have no conflicts of interest.

Authors' Contributions

XZ and XC completed the drawing of the picture and the writing part of the content. XZ and XC contributed equally to this work. ZL, BY, YZ, SP, YH, and DH provided support for content writing and data analysis. YZ and CL conceived and supervised the writing of this article.

Acknowledgments

This work was supported by the Scientific Research Project (2019) of Health Commission of Hunan (B2019200), Natural Science Foundation of Hunan Province (2022JJ31024), and Science and Technology Project of Zhuzhou (2020-006).

References

- [1] A. P. Becker, B. E. Sells, S. J. Haque, and A. Chakravarti, "Tumor heterogeneity in glioblastomas: from light microscopy to molecular pathology," *Cancers*, vol. 13, 2021.
- [2] R. Chen, M. Smith-Cohn, A. L. Cohen, and H. Colman, "Glioma subclassifications and their clinical significance," *Neurotherapeutics*, vol. 14, no. 2, pp. 284–297, 2017.
- [3] C. Hanna, T. A. Lawrie, E. Rogozińska et al., "Treatment of newly diagnosed glioblastoma in the elderly: a network meta-analysis," *Cochrane Database of Systematic Reviews*, vol. 3, Article ID Cd013261, 2020.
- [4] F. Di Cintio, M. Dal Bo, L. Baboci, E. De Mattia, M. Polano, and G. Toffoli, "The molecular and microenvironmental landscape of glioblastomas: implications for the novel treatment choices," *Frontiers in Neuroscience*, vol. 14, Article ID 603647, 2020.
- [5] Q. T. Ostrom, N. Patil, G. Cioffi, K. Waite, C. Kruchko, and J. S. Barnholtz-Sloan, "CBTRUS statistical report: primary brain and other central nervous system tumors diagnosed in the United States in 2013-2017," *Neuro-Oncology*, vol. 22, no. Supplement_1, pp. iv1–iv96, 2020.
- [6] M. Ferguson, G. Rodrigues, J. Cao, and G. Bauman, "Management of high-grade gliomas in the elderly," *Seminars in Radiation Oncology*, vol. 24, no. 4, pp. 279–288, 2014.
- [7] A. Calcinotto, J. Kohli, E. Zagato, L. Pellegrini, M. Demaria, and A. Alimonti, "Cellular senescence: aging, cancer, and injury," *Physiological Reviews*, vol. 99, no. 2, pp. 1047–1078, 2019.
- [8] L. H. Chen, J. F. Liu, Y. Lu, Xy He, C. Zhang, and Hh Zhou, "Complement C1q (C1qA, C1qB, and C1qC) may Be a potential prognostic factor and an index of tumor microenvironment remodeling in osteosarcoma," *Frontiers Oncology*, vol. 11, Article ID 642144, 2021.
- [9] B. Chen, M. S. Khodadoust, C. L. Liu, A. M. Newman, and A. A. Alizadeh, "Profiling tumor infiltrating immune cells with CIBERSORT," *Methods in Molecular Biology*, vol. 1711, pp. 243–259, 2018.
- [10] C. L. Brinkmeyer-Langford, J. Guan, G. Ji, and J. J. Cai, "Aging shapes the population-mean and -dispersion of gene expression in human brains," *Frontiers in Aging Neuroscience*, vol. 8, p. 183, 2016.
- [11] M. Fane and A. T. Weeraratna, "How the ageing microenvironment influences tumour progression," *Nature Reviews Cancer*, vol. 20, no. 2, pp. 89–106, 2020.
- [12] M. I. Fonseca, S. H. Chu, M. X. Hernandez et al., "Cell-specific deletion of C1qa identifies microglia as the dominant source of C1q in mouse brain," *Journal of Neuroinflammation*, vol. 14, no. 1, p. 48, 2017.
- [13] T. D. Purves-Tyson, K. Robinson, A. M. Brown et al., "Increased macrophages and C1qA, C3, C4 transcripts in the midbrain of people with schizophrenia," *Frontiers in Immunology*, vol. 11, p. 2002, 2020.
- [14] J. Wang, B. Li, C. Wang, Y. Luo, M. Zhao, and P. Chen, "Long noncoding RNA FOXD2-AS1 promotes glioma cell cycle progression and proliferation through the FOXD2-AS1/miR-31/CDK1 pathway," *Journal of Cellular Biochemistry*, vol. 120, no. 12, Article ID 19784, 2019.
- [15] Z. Song, Y. Pan, G. Ling et al., "Escape of U251 glioma cells from temozolomide-induced senescence was modulated by CDK1/survivin signaling," *Am J Transl Res*, vol. 9, no. 5, pp. 2163–2180, 2017.
- [16] P. J. McLaughlin, B. Bakall, J. Choi et al., "Lack of fibulin-3 causes early aging and herniation, but not macular degeneration in mice," *Human Molecular Genetics*, vol. 16, no. 24, pp. 3059–3070, 2007.
- [17] M. Tasaki, M. Ueda, Y. Hoshii et al., "A novel age-related venous amyloidosis derived from EGF-containing fibulin-like extracellular matrix protein 1," *The Journal of Pathology*, vol. 247, no. 4, pp. 444–455, 2019.
- [18] Y. Hu, P. D. Pioli, E. Siegel et al., "EFEMP1 suppresses malignant glioma growth and exerts its action within the tumor extracellular compartment," *Molecular Cancer*, vol. 10, no. 1, p. 123, 2011.
- [19] D. Lei, F. Zhang, D. Yao, N. Xiong, X. Jiang, and H. Zhao, "MiR-338-5p suppresses proliferation, migration, invasion,

- and promote apoptosis of glioblastoma cells by directly targeting EFEMP1,” *Biomedicine & Pharmacotherapy*, vol. 89, pp. 957–965, 2017.
- [20] S. Zhang, Z. Ye, X. Song et al., “Association of EFEMP1 gene polymorphisms with the risk of glioma: a hospital-based case-control study in a Chinese Han population,” *Journal of the Neurological Sciences*, vol. 349, no. 1-2, pp. 54–59, 2015.
- [21] Z. Li and F. Picard, “Modulation of IGFBP2 mRNA expression in white adipose tissue upon aging and obesity,” *Hormone and Metabolic Research*, vol. 42, no. 11, pp. 787–791, 2010.
- [22] D. Hu, L. Pawlikowska, A. Kanaya et al., “Serum insulin-like growth factor-1 binding proteins 1 and 2 and mortality in older adults: the Health, Aging, and Body Composition Study,” *Journal of the American Geriatrics Society*, vol. 57, no. 7, pp. 1213–1218, 2009.
- [23] M. Sunderić, N. Mihailović, and O. Nedić, “Protein molecular forms of insulin-like growth factor binding protein-2 change with aging,” *Experimental Gerontology*, vol. 58, pp. 154–158, 2014.
- [24] Y. Lin, T. Jiang, K. Zhou et al., “Plasma IGFBP-2 levels predict clinical outcomes of patients with high-grade gliomas,” *Neuro-Oncology*, vol. 11, no. 5, pp. 468–476, 2009.
- [25] Y. Liu, F. Li, Y. T. Yang et al., “IGFBP2 promotes vasculogenic mimicry formation via regulating CD144 and MMP2 expression in glioma,” *Oncogene*, vol. 38, no. 11, pp. 1815–1831, 2019.
- [26] S. S. Patil, R. Railkar, M. Swain, H. S. Atreya, R. R. Dighe, and P. Kondaiah, “Novel anti IGFBP2 single chain variable fragment inhibits glioma cell migration and invasion,” *Journal of Neuro-Oncology*, vol. 123, no. 2, pp. 225–235, 2015.
- [27] J. Cai, Q. Chen, Y. Cui et al., “Immune heterogeneity and clinicopathologic characterization of IGFBP2 in 2447 glioma samples,” *OncoImmunology*, vol. 7, no. 5, Article ID e1426516, 2018.
- [28] C. Song, F. Shen, Y. Liu, J. Zhang, and S. Wei Song, “IGFBP2 promotes neural stem cell maintenance and proliferation differentially associated with glioblastoma subtypes,” *Brain Research*, vol. 1704, pp. 174–186, 2019.
- [29] T. Li, M. E. Forbes, G. N. Fuller, J. Li, X. Yang, and W. Zhang, “IGFBP2: integrative hub of developmental and oncogenic signaling network,” *Oncogene*, vol. 39, no. 11, pp. 2243–2257, 2020.
- [30] L. M. Moore, K. M. Holmes, S. M. Smith et al., “IGFBP2 is a candidate biomarker for Ink4a-Arf status and a therapeutic target for high-grade gliomas,” *Proceedings of the National Academy of Sciences of the United States of America*, vol. 106, no. 39, pp. 16675–16679, 2009.
- [31] Q. Guo, X. Xiao, and J. Zhang, “MYD88 is a potential prognostic gene and immune signature of tumor microenvironment for gliomas,” *Frontiers Oncology*, vol. 11, Article ID 654388, 2021.
- [32] Y. Tian, Y. Ke, and Y. Ma, “High expression of stromal signatures correlated with macrophage infiltration, angiogenesis and poor prognosis in glioma microenvironment,” *PeerJ*, vol. 8, Article ID e9038, 2020.
- [33] M. B. Pereira, L. R. C. Barros, P. A. Bracco et al., “Transcriptional characterization of immunological infiltrates and their relation with glioblastoma patients overall survival,” *OncoImmunology*, vol. 7, no. 6, Article ID e1431083, 2018.
- [34] S. J. Galli and M. Tsai, “Mast cells: versatile regulators of inflammation, tissue remodeling, host defense and homeostasis,” *Journal of Dermatological Science*, vol. 49, no. 1, pp. 7–19, 2008.
- [35] M. Prośniak, L. A. Harshyne, D. W. Andrews et al., “Glioma grade is associated with the accumulation and activity of cells bearing M2 monocyte markers,” *Clinical Cancer Research*, vol. 19, no. 14, pp. 3776–3786, 2013.
- [36] M. G. Morvan and L. L. Lanier, “NK cells and cancer: you can teach innate cells new tricks,” *Nature Reviews Cancer*, vol. 16, no. 1, pp. 7–19, 2016.
- [37] I. Golán, L. Rodríguez de la Fuente, and J. A. Costoya, “NK cell-based glioblastoma immunotherapy,” *Cancers*, vol. 10, 2018.
- [38] S. Wu, W. Yang, H. Zhang et al., “The prognostic landscape of tumor-infiltrating immune cells and immune checkpoints in glioblastoma,” *Technology in Cancer Research and Treatment*, vol. 18, Article ID 153303381986994, 2019.
- [39] A. J. Gentles, A. M. Newman, C. L. Liu et al., “The prognostic landscape of genes and infiltrating immune cells across human cancers,” *Nature Medicine*, vol. 21, no. 8, pp. 938–945, 2015.
- [40] C. Gu-Trantien and K. Willard-Gallo, “PD-1(hi)CXCR5(-) CD4(+) T(FH) cells play defense in cancer and offense in arthritis,” *Trends in Immunology*, vol. 38, no. 12, pp. 875–878, 2017.
- [41] S. Ning, J. Wu, Y. Pan, K. Qiao, L. Li, and Q. Huang, “Identification of CD4+ conventional T cells-related lncRNA signature to improve the prediction of prognosis and immunotherapy response in breast cancer,” *Frontiers in Immunology*, vol. 13, Article ID 880769, 2022.
- [42] K. I. Woroniecka, K. E. Rhodin, P. Chongsathidkiet, K. A. Keith, and P. E. Fecci, “T-Cell dysfunction in glioblastoma: applying a new framework,” *Clinical Cancer Research*, vol. 24, no. 16, pp. 3792–3802, 2018.
- [43] C. Banissi, F. Ghiringhelli, L. Chen, and A. F. Carpentier, “Treg depletion with a low-dose metronomic temozolomide regimen in a rat glioma model,” *Cancer Immunology, Immunotherapy*, vol. 58, no. 10, pp. 1627–1634, 2009.
- [44] L. Vandenberg and S. W. Van Gool, “Treg infiltration in glioma: a hurdle for anti-glioma immunotherapy,” *Immunotherapy*, vol. 4, no. 7, pp. 675–678, 2012.
- [45] M. L. Broekman, S. L. N. Maas, E. R. Abels, T. R. Mempel, A. M. Krichevsky, and X. O. Breakefield, “Multidimensional communication in the microenvirons of glioblastoma,” *Nature Reviews Neurology*, vol. 14, no. 8, pp. 482–495, 2018.